δ-phase precipitation regularity of cold-rolled fine-grained GH4169 alloy plate and its effect on mechanical properties

Hao XUE[1], Jing-qi ZHAO[1], Yong-kang LIU[1], Chun-xiang ZHANG[2], Jun-ting LUO[1,2]

1. Key Laboratory of Advanced Forging & Stamping Technology and Science of Ministry of Education,
Yanshan University, Qinhuangdao 066004, China;
2. State Key Laboratory of Metastable Materials Science and Technology,
Yanshan University, Qinhuangdao 066004, China

Abstract: Cold rolling and heat-treatment were used for the grain refinement of GH4169 superalloy plate. The effects of cold rolling reduction ratio and heat-treatment time on the precipitated δ phase, and the effects of δ-phase content and morphology on the mechanical properties of the GH4169 alloy plates, are studied. The results demonstrate that cold-rolling can promote the precipitation of the δ phase and its transformation from the δ-Ni_3Nb phase to the δ-$NbNi_4$ phase. The comprehensive properties of the alloy are better when the heat treatment time is 1 h, with 132 MPa increase in the tensile strength and only 2.9% decrease in the elongation relative to those of the original material. The mechanical properties of the alloy are shown to change greatly with the change in the δ-phase morphology.
Key words: fine-grained GH4169 alloy; cold rolling; δ phase; mechanical properties

1 Introduction

The GH4169 (Inconel 718) superalloy is a Ni−Cr−Fe deformation alloy with high strength, strong oxidation resistance, good hot workability, and a stable high-temperature microstructure [1−3]. It is widely used to manufacture high-temperature materials, especially the heat-resistant components of aircraft and solid rockets [4−6]. The aging treatment of the GH4169 superalloy solid solution produces austenite matrix (γ phase) in its interior, along with γ′ phase (strengthening phase) and γ″ phase. δ phase also precipitates inside the grains or at grain boundary under specific conditions, and a small amount of NbC and TiN may be mixed [7−9]. The morphology, content, and distribution of the δ phase significantly influence the hot-working deformation behavior and mechanical properties of the GH4169 superalloy during service [10,11]. Hence, by controlling the morphology and content of the δ phase during deformation and heat treatment, the grain growth of the alloy can be effectively controlled to achieve grain refinement and improve the performance of the alloy [12,13].

The mechanical properties of the GH4169 alloy depend on its microstructural conditions, including the phase composition, phase content and morphology of each phase. The content and morphology of the δ phase significantly influence the comprehensive mechanical properties of the alloy, so studying the precipitation regularity of the δ phase during heat treatment is important [14]. A large number of studies have shown that the precipitation temperature of the δ phase is 780−980 °C, and the temperature range of the fastest precipitation is generally considered to be 890−900 °C [15,16]. RAFIEI et al [17] reported

that the activation energy of δ phase formation with transformation fraction of 0.5% and 50% during aging (212.4 and 197.5 kJ/mol) was similar to that of Nb diffusion in Ni ((202.59±4.71) kJ/mol). Therefore, they concluded that the microscopic mechanism of δ-phase formation is the diffusion of Nb in the matrix. YE et al [18] investigated the effect of the δ-phase content on the mechanical properties of the GH4169 alloy at room temperature. As the δ-phase content increased from 2.20 to 5.21 wt.%, the yield strength of the GH4169 alloy was increased by 61 MPa, and its tensile strength was increased by 78 MPa. With further increasing δ-phase content from 2.20 to 7.56 wt.%, the elongation of the alloy was decreased by 14.1%. In addition, NING et al [19] reported that the rod-shaped δ phase is beneficial to improving the plasticity of the alloy, and that the needle-shaped δ phase is helpful for improving the strength of the alloy. They also verified that dislocation motion and atomic diffusion are the fundamental reasons for δ-phase precipitation. CHEN et al [20] investigated the effect of different δ-phase volume fractions on the fatigue properties of alloys at room temperature, and found almost no effect on the fatigue life when the strain amplitude was higher than 0.5%. However, at a strain amplitude of 0.4%, the fatigue life of the alloy was found to increase with the increasing volume fraction of the δ phase.

The majority of studies have been focused on the influence of temperature on the precipitation of the δ phase, and there are few reports on the influence of heat treatment time on the precipitation regularity of the δ phase. In the present study, the effects of different cold-rolling reduction ratios and heat treatment time on the regularity of the δ phase precipitation are investigated. The effects of the δ phase on the tensile strength and elongation of the GH4169 alloy are also examined via tensile tests. Then, the δ-phase precipitation law in the GH4169 alloy is revealed, and a specific approach for the preparation of the GH4169 alloy is provided.

2 Experimental

To study the influence of cold rolling deformation on the precipitation of the δ phase, an original plate of GH4169 alloy with the thickness of 3 mm was divided into three groups of samples which were then cold-rolled to thicknesses of 2.4,

1.8 and 1.2 mm, giving thickness reductions of 20%, 40% and 60%, respectively. The cold-rolled samples and a sample without reduction were then subjected to δ-phase precipitation at 900 °C for 10 h. The process parameters are presented in Table 1.

Table 1 Process parameters of cold rolling of GH4169 alloy

Reduction ratio/%	Heat-treatment temperature/°C	Heat-treatment time/h
0	900	10
20	900	10
40	900	10
60	900	10

To study the influence of different heat treatment time on the precipitation of the δ phase, the original plates were divided into five groups, which were then heat-treated at 900 °C in an ARCHIMEDES VF1600 vacuum heating furnace for 1, 5, 10, 20 and 40 h. Water quenching was performed immediately after the precipitation.

The microstructure of the GH4169 alloy plate was determined with a Zeiss optical microscope. First, the sample was sanded and mechanically polished, and then etched with an etchant comprising 10 mL of HNO_3, 50 mL of H_2O, 40 mL of HCl, and 2.5 g of $CuCl_2$. The δ phase in the matrix was calibrated using the Linksys32 phase analysis software, and the ratio of the area of the δ phase to that of the matrix was calculated.

The phase composition and content of the GH4169 alloy samples were tested with a D/Max−2500/PC X-ray diffractometer (XRD). The sample was ground, mechanically polished, and ultrasonically cleaned before the XRD examination to remove any residual stress on the sample surface and ensure the accuracy of the results.

The SEM microstructure of the GH4169 alloy under different heat treatment time was analyzed with a Hitachi S−4800 scanning electron microscope (SEM). The δ phase of the GH4169 alloy was analyzed via energy disperse spectroscopy (EDS) using a Horiba 7593−H spectrometer attached to the Hitachi S−4800 scanning electron microscope. The microstructure of the GH4169 alloy was observed with a JEM−2010 transmission electron microscope (TEM).

3 Results

3.1 Precipitation regularity

The energy spectrum analysis of the sample without reduction after heat treatment at 900 °C for 10 h is presented in Fig. 1. The composition of the selected test location, which lies within the δ phase, is listed in Table 2. Thus, the test location is seen to contain 43.77 at.% Ni and 14.59 at.% Nb, which is consistent with the composition of the δ-Ni$_3$Nb phase. The microstructures of the GH4169 alloy after different cold rolling reduction ratios followed by heat treatment at 900 °C for 10 h are presented in Fig. 2. Here, the sample without reduction (Fig. 2(a)) exhibits fine needle-like δ phases at the grain boundaries, along with some inward growth of the δ phase to form a staggered arrangement [21]. By contrast, the 20% cold-rolled sample in Fig. 2(b)
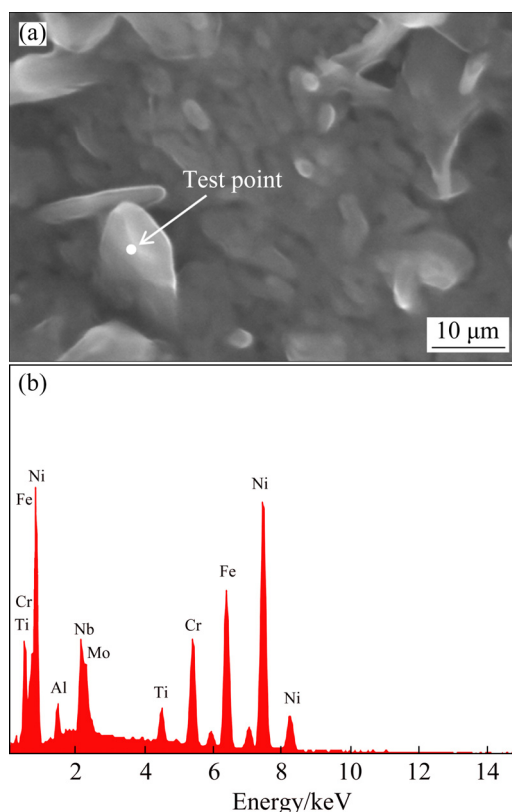
Fig. 1 EDS results of sample without reduction after heat treatment at 900 °C for 10 h

Table 2 Composition of δ phase in sample without reduction after heat treatment at 900 °C for 10 h (at.%)

Al	Ti	Cr	Fe	Ni	Nb	Mo
4.64	3.23	12.66	19.2	43.77	14.59	2.1

displays a remarkably improved δ-phase content, although only some of the crystal grains are completely covered by the precipitated δ phase. The 40% cold-rolled sample subjected to δ-phase precipitation treatment is shown in Fig. 2(c), where the additional reduction in thickness is seen to result in increased grain deformation and the formation of a band structure. With further cold rolling (60% thickness reduction), the δ-phase content of the sample in Fig. 2(d) is only slightly more than that of the 40% cold-rolled sample. However, the δ phase is seen to be more uniform and neatly arranged inside the deformed strip-shaped grains.

The XRD patterns of the GH4169 alloy after cold rolling with different reduction ratios followed by heat treatment at 900 °C for 10 h are presented in Fig. 3. Here, the sample without reduction subjected to heat treatment is seen to exhibit only the (201) and (211) diffraction peaks of the δ phase, which are characteristic peaks of the δ-Ni$_3$Nb phase. By contrast, the XRD patterns of the cold-rolled samples display the (020), (012) and (013) diffraction peaks of the δ-NbNi$_4$ phase, and the intensity of these peaks is seen to increase with increasing cold-rolling reduction ratio. The volume fractions of the δ-Ni$_3$Nb and δ-NbNi$_4$ phases in the GH4169 alloy with different cold rolling reduction ratios were determined via the quantitative X-ray phase analysis, and the results are presented in Table 3. Here, it can be seen that the volume fraction of the δ phase increases as the sample thickness is reduced, but this increasing trend becomes less significant with larger thickness reduction. Thus, the 60% cold-rolled alloy displays a smaller volume fraction increment in the δ phase than the 40% cold-rolled alloy, which is consistent with the metallographic microscopy results shown in Fig. 2.

The sample without reduction contains only the δ-Ni$_3$Nb phase, while the cold-rolled samples contain both the δ-NbNi$_4$ and δ-Ni$_3$Nb phases. Further, the proportion of the δ-Ni$_3$Nb phase is seen to decrease with the increase of cold-rolling reduction ratio up to 60%, at which the characteristic (211) peak of the δ-Ni$_3$Nb phase has disappeared.

The above analysis indicates that the increase in the amount of cold rolling reduction can increase the nucleation rate of the δ phase and reduce its
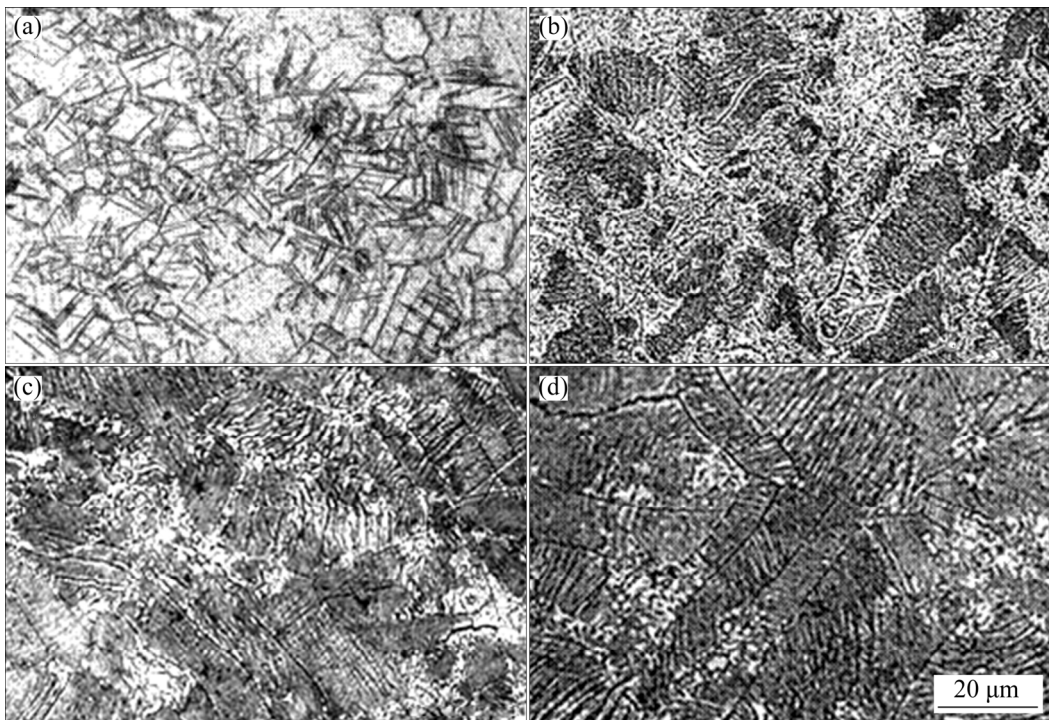
Fig. 2 Morphologies of δ phase in GH4169 alloy plates with different cold-rolling reduction ratios: (a) 0%; (b) 20%; (c) 40%; (d) 60%
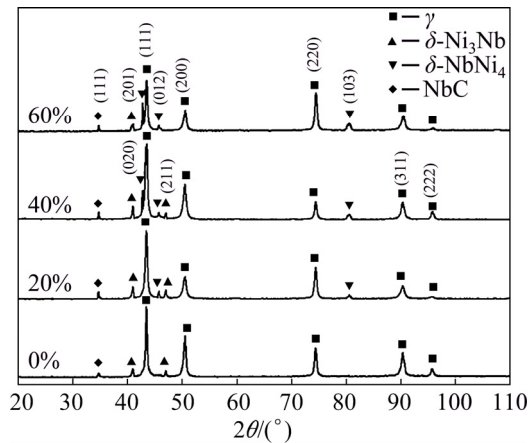
Fig. 3 XRD patterns of GH4169 alloy plates with different cold-rolling reduction ratios

Table 3 Contents of δ-Ni$_3$Nb phase and δ-NbNi$_4$ phase in GH4169 alloy plates with different cold-rolling reduction ratios

| Reduction ratio/%	Content/vol.%		
	δ phase	δ-Ni$_3$Nb	δ-NbNi$_4$
0	6.14	6.14	0
20	9.15	4.13	5.02
40	10.20	2.84	7.66
60	10.80	2.30	8.50

critical nucleation work, thereby promoting the precipitation of the δ phase and improving the uniformity of the δ-phase distribution. At the same time, cold rolling deformation can improve the internal distortional energy of the alloy and promote the transformation of the δ-Ni$_3$Nb phase to the δ-NbNi$_4$ phase. In other words, cold rolling deformation can promote the precipitation of the δ-NbNi$_4$ phase.

The relative area fractions and average aspect ratios of the GH4169 samples subjected to heat treatment at 900 °C for different time are presented in Table 4, and the corresponding microstructures are indicated in Fig. 4. After heat treatment of the

Table 4 Relative area fractions and average aspect ratios of δ-phase in GH4169 alloy plate heat-treated at 900 °C for different time

Heat-treatment time/h	Relative area fraction/%	Average aspect ratio
1	2.35	8.74
5	5.46	18.35
10	10.21	29.78
20	16.33	8.03
40	19.58	6.43
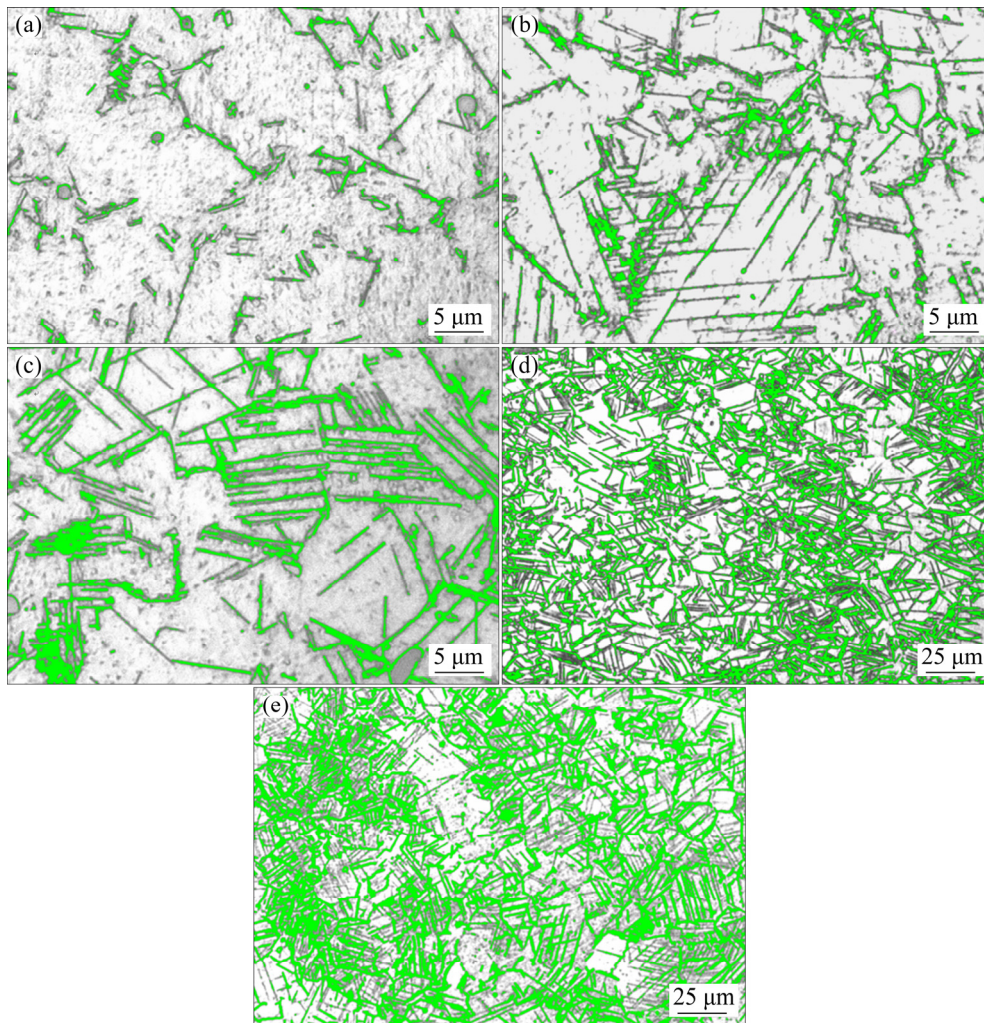
Fig. 4 Microstructures of GH4169 alloy plates heat-treated at 900 °C for different time: (a) 1 h; (b) 5 h; (c) 10 h; (d) 20 h; (e) 40 h

GH4169 alloy plate at 900 °C for 1 h, the δ phase initially precipitates at grain boundaries and then shows a fine acicular structure. The average aspect ratio of the δ phase is 8.74, but its relative content is very little and the relative area fraction of the δ phase is only 2.35%. By contrast, the heat treatment at 900 °C for 5 h results in the precipitation of a large amount of acicular δ phase at grain boundaries, and the appearance of the staggering of the δ phase in some grains. Moreover, the average aspect ratio of the δ phase is increased to 18.35, and the relative area fraction is increased to 5.46%. After heat treatment at 900 °C for 10 h, the relative area fraction of the δ phase is further increased to 10.21%, and the staggered acicular δ phase (with an increased average aspect ratio of 29.78) is seen to be densely distributed. After 20 h at 900 °C, the area fraction of the δ phase is increased to 16.33%

and is seen to be evenly distributed over the entire matrix. However, the average aspect ratio of the δ phase is seen to decrease to 8.03 because the longitudinal growth of each phase is now hindered by the presence of the interlaced δ phase, and hence the δ phase begins to grow laterally and transforms into a rod-like structure. Finally, after 40 h at 900 °C, the area fraction of δ-phase is slightly increased to 19.58%, and the rod-like acicular δ phase is seen to be densely distributed with an average aspect ratio of 6.43, while the staggering is also pronounced and evenly distributed inside the matrix. Compared with the results of 20 h heat treatment, however, the increasing rate of the proportion of the δ phase is seen to decrease due to the decrease in Nb content [22].
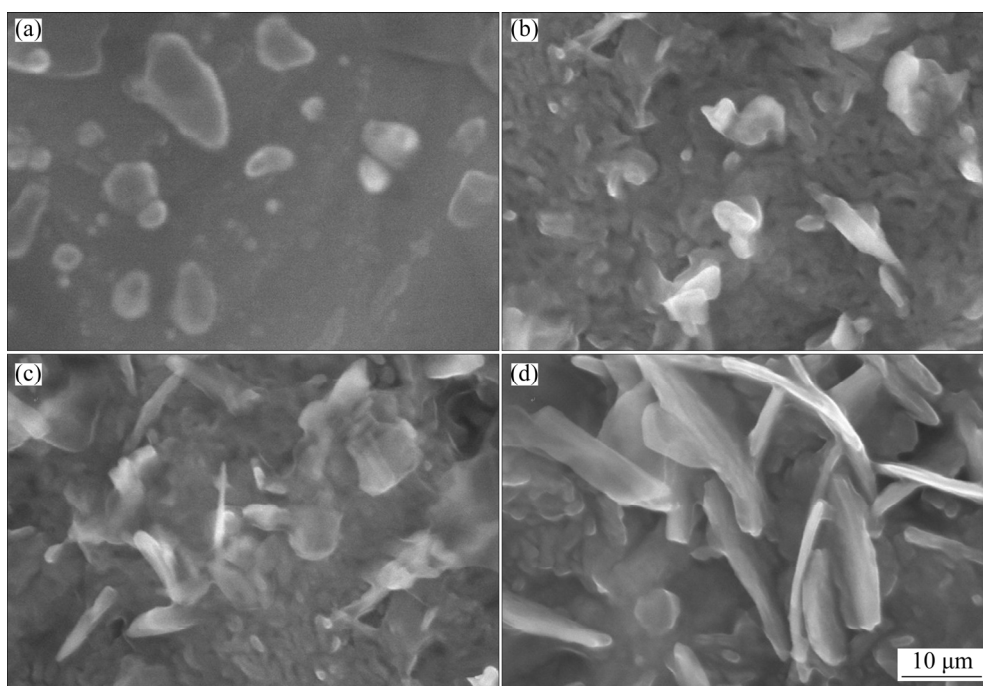
The SEM images of the GH4169 alloy plates after different heat treatment time at 900 °C are

presented in Fig. 5. Thus, after 1 h, the δ phase is seen to present fine particles with a tendency of longitudinal elongation (Fig. 5(a)). After 5 h, however, the δ phase begins to take an acicular structure (Fig. 5(b)). After 20 h, a large number of the δ phases are seen to intersect and the presence of a distinct acicular δ phase is observed (Fig. 5(c)). Finally, after 40 h, the δ phase is seen to grow into a long rod-like morphology in which individual rods crisscross to become intertwined and twisted (Fig. 5(d)). Consequently, the plasticity of the alloy is deteriorated.
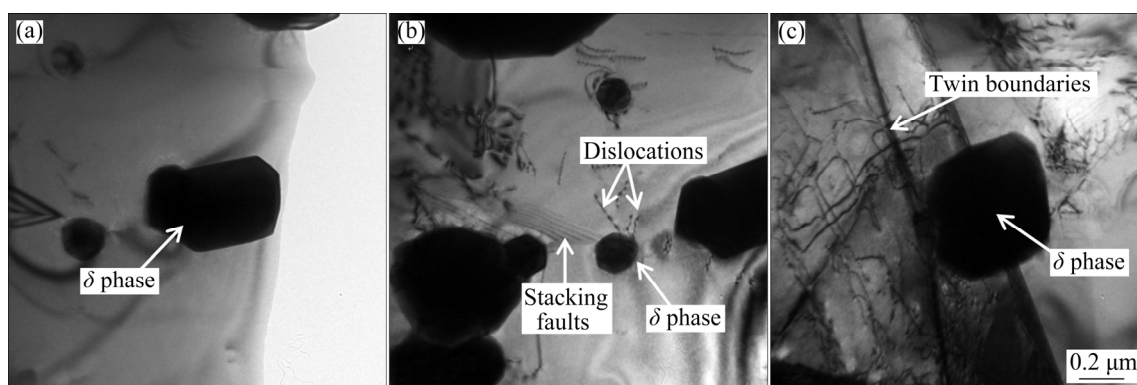
The TEM images of different regions of the GH4169 alloy after heat treatment at 900 °C for 1 h are presented in Fig. 6. The δ phase is seen to initially precipitate from the grain boundary and the twin boundary in the form of fine particles (Figs. 6(a, c)). With prolonging heat treatment time, however, the δ phase is seen to grow into a fine acicular morphology, and dislocations become entangled around the δ phase, which hinders the dislocation motion and improves the alloy strength (Fig. 6(b)). In addition, the γ'' phase is seen to become distorted during precipitation, thus further generating stacking faults [23,24]. The δ phase is generated by the γ'' phase transition [25]. Hence, a stacking fault is observed near the δ phase in Fig. 6(b).

The XRD diffraction patterns of the GH4169 alloy plates subjected to different heat treatment time at 900 °C are presented in Fig. 7. Here, the peak intensity of the δ-phase is seen to increase

Fig. 5 SEM images of GH4169 alloy plates heat-treated at 900 °C for different time: (a) 1 h; (b) 5 h; (c) 20 h; (d) 40 h

Fig. 6 TEM images of different regions in GH4169 alloy plates after heat treatment at 900 °C for 1 h
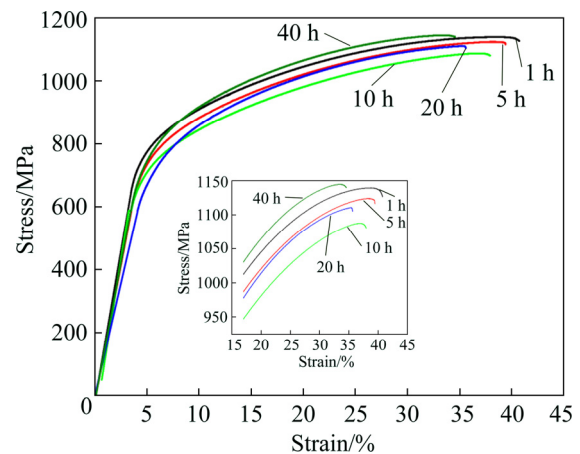
Fig. 7 XRD patterns of GH4169 alloy plates heat-treated at 900 °C for different time
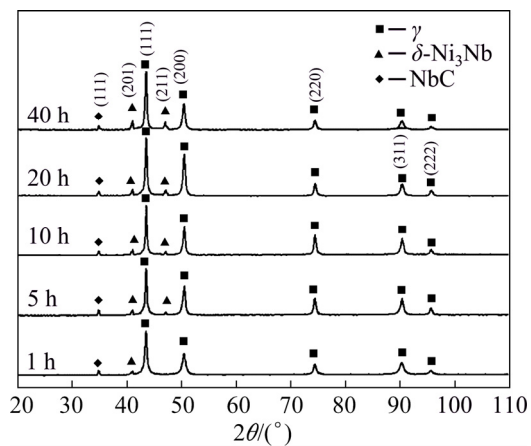
Fig. 8 Tensile stress−strain curves of GH4169 alloy plates heat-treated at 900 °C for different time

with increasing heat treatment time. This is primarily attributed to a gradual decrease in the content of the γ phase, which is a member of the γ'' phase, as it transforms into the corresponding equilibrium form, i.e. the δ phase, during the precipitation process [26]. In comparison with the cold-rolled plate (Fig. 3), the alloy plate after δ-phase precipitate treatment (Fig. 7) contains only the δ-Ni$_3$Nb phase and does not contain any δ-NbNi$_4$ phase. Hence, the prolongation of heat treatment time alone does not provide sufficient energy to convert the δ-Ni$_3$Nb phase into the δ-NbNi$_4$ phase, but rolling before heat treatment can effectively promote this transformation.

3.2 Mechanical properties

The tensile curves of the GH4169 alloy plates after heat treatment at 900 °C for different time are presented in Fig. 8, and the corresponding mechanical properties are listed in Table 5. These results confirm that the content of the δ phase progressively increases with increasing heat treatment time, while the tensile strength of the alloy initially decreases (but remains higher than that of the original material) and subsequently increases, and the elongation continually decreases. After 1 h heat treatment, the overall performance of the alloy is seen to be improved, with a tensile strength of 1140 MPa (i.e., 132 MPa higher than that of the original material) and elongation only 2.9% lower than that of the original material. After heating for 5 h, however, the tensile strength and elongation of the GH4169 alloy plate are seen to decrease. Nevertheless, after 10 h heat treatment,

Table 5 Mechanical properties of GH4169 alloy plates heat-treated at 900 °C for different time

Heat-treatment time/h	Content of δ phase/vol.%	Elongation/ %	Tensile strength/MPa
0	–	43.6	1008
1	2.18	40.7	1140
5	4.00	39.4	1124
10	6.14	37.4	1087
20	8.66	34.8	1110
40	9.50	33.7	1145

the tensile strength of the alloy is seen to increase, by only 79 MPa, while the elongation is decreased by 6.2%, compared to the original material. As seen from Fig. 4, the δ phase becomes gradually coarser with increasing heat treatment time, which would reduce the pinning effect of the δ phase [11] and allow the grain to grow rapidly. Therefore, the strength and plasticity of the material would decrease, thus resulting in the above phenomenon. At heat treatment for 20 h, the tensile strength of the material is seen to increase, but the plasticity continues to decrease. After heating for 40 h, the tensile strength of the material is increased by 137 MPa compared to that of the original material, but the plasticity becomes extremely poor and the elongation is decreased by about 10% compared to that of the original material. An examination of the micrograph in Fig. 4 indicates that the heat treatment for 20 h results in a large number of acicular δ phases which are evenly distributed on the substrate and are interlaced with each other, thus making it difficult for grains to slide, and hence

improving the tensile strength of the material. However, due to the poor plasticity of the δ phase relative to the substrate [27,28], the development of a large number of δ phases leads to a significant decrease in the plasticity of the material.

In summary, the content and morphology of the δ phase play a decisive role in the mechanical properties of the GH4169 alloy. During heat treatment, the precipitation of a small quantity of the high-temperature δ phase contributes to grain refining by pinning the grain boundaries [29,30]. However, the inevitable coarsening of the δ phase with longer heat-treatment time leads to a reduction in this pinning effect, and with the further increase in the δ-phase content, the elongation of the material is greatly reduced.

4 Conclusions

(1) Cold rolling is shown to increase the nucleation rate of the δ phase and reduce its critical nucleation work, thereby promoting the precipitation of the δ phase and its transformation from the δ-Ni$_3$Nb phase to the δ-NbNi$_4$ phase. The heat-treatment time is shown to have an important influence on the δ-phase content and morphology of the GH4169 alloy.

(2) After heat treatment for different time, the tensile strength of the alloy is always higher than that of the original material. After heat treatment for 1 h, the comprehensive properties of the alloy are enhanced and the tensile strength is 132 MPa higher than that of the original material. When the heat-treatment time is extended to 20 or 40 h, the tensile strength of the material is further improved because the cross-distribution of the δ phase inhibits the sliding of the grains, but this is accompanied by an extreme reduction in the elongation.

References

[1]   XU Xiao-yan, MA Xiang-dong, WANG Hong, YE Zhang, CHANG Jian-wei, XU Yao, SUN Guang-ai, LÜ Wei-jie, GAO Yu-kui. Characterization of residual stresses and microstructural features in an Inconel 718 forged compressor disc [J]. Transactions of Nonferrous Metals Society of China, 2019, 29: 569−578.

[2]   XIAO Wei-han, LU Shi-qiang, WANG Ya-chao, SHI Jing. Mechanical and tribological behaviors of graphene/Inconel 718 composites [J]. Transactions of Nonferrous Metals Society of China, 2018, 28: 1958−1969.

[3]   HERNÁNDEZ M, AMBRIZ R R, CORTÉS R, GÓMORA C M, PLASCENCIA G, JARAMILLO D. Assessment of gas tungsten arc welding thermal cycles on Inconel 718 alloy [J]. Transactions of Nonferrous Metals Society of China, 2019, 29: 579−587.

[4]   DU Jin-hui, LU Xu-dong, QUN Deng, BI Zhong-nan. Progress in the research and manufacture of GH4169 alloy [J]. Journal of Iron and Steel Research International, 2015, 22: 657−663.

[5]   POLLOCK T M, TIN S. Nickel-based superalloys for advanced turbine engines: Chemistry, microstructure and properties [J]. Journal of Propulsion and Power, 2006, 22(2): 361−374.

[6]   ZHANG Xin, LI Hong-wei, ZHAN Mei. Mechanism for the macro and micro behaviors of the Ni-based superalloy during electrically-assisted tension: Local Joule heating effect [J]. Journal of Alloys and Compounds, 2018, 742: 480−489.

[7]   MA T J, CHEN X F, LI W Y, YANG X M, ZHANG Y, YANG S Q. Microstructure and mechanical property of linear friction welded nickel-based superalloy joint [J]. Materials and Design, 2016, 89: 85−93.

[8]   AN X L, ZHANG B M, CHU C L, ZHOU L, CHU P K. Evolution of microstructures and properties of the GH4169 superalloy during short-term and high-temperature processing [J]. Materials Science and Engineering A, 2019, 744: 255−266.

[9]   ANBARASAN N, GUPTA B K, PRAKASH S, MUTHUKUMAR P, OYYARAVELU R, KUMAR R J F, JEROME S. Effect of heat treatment on the microstructure and mechanical properties of Inconel 718 [J]. Material Today, 2018, 5(2): 7716−7724.

[10]   HUANG Rong-shen, SUN Yong-an, XING Lei-lei, SONG Guo-lin, LIU Wei, LI Qiu-lin. Effect of gradient microstructure pinned by δ phase on elevated temperature performances of GH4169 [J]. Materials Science and Engineering A, 2013, 582: 368−373.

[11]   ANDERSON M, THIELIN A L, BRIDIER F, BOCHER P, SAVOIE J. δ phase precipitation in Inconel 718 and associated mechanical properties [J]. Materials Science and Engineering A, 2017, 679: 48−55.

[12]   LUO Jun-ting, YU Wen-lu, XI Chen-yang, ZHANG Chun-xiang, MA Chun-hui. Preparation of ultrafine-grained GH4169 superalloy by high-pressure torsion and analysis of grain refinement mechanism [J]. Journal of Alloys and Compounds, 2019, 777: 157−164.

[13]   WEN D X, LIN Y C, ZHOU Y. A new dynamic recrystallization kinetics model for a Nb containing Ni−Fe−Cr-base superalloy considering influences of initial δ phase [J]. Vacuum, 2017, 141: 316−327.

[14]   JAWAHIR I S, KAYNAK Y, LU Tao. The impact of novel material processing methods on component quality life and performance [J]. Procedia CIRP, 2014, 22: 33−44.

[15]   ZHANG Hong-jun, LI Chong, LIU Yong-chang, GUO Qian-ying, HUANG Yuan, LI Hui-jun, YU Jian-xin. Effect of hot deformation on γ'' and δ phase precipitation of Inconel 718 alloy during deformation and isothermal treatment [J]. Journal of Alloys and Compounds, 2017, 716: 65−72.

[16]   AZADIAN S, WEI Liu-ying, WARREN R. δ phase precipitation in Inconel 718 [J]. Materials Characterization, 2004, 53(1): 7−16.

[17] RAFIEI M, MIRZADEH H, MALEKAN M. Micro-mechanisms and precipitation kinetics of delta (δ) phase in Inconel 718 superalloy during aging [J]. Journal of Alloys and Compounds, 2019, 795: 207−212.

[18] YE Neng-yong, CHENG Ming, ZHANG Shi-hong, SONG Hong-wu, ZHOU Hong-wei, WANG Ping-bo. Effect of δ phase on mechanical properties of GH4169 alloy at room temperature [J]. Journal of Iron and Steel Research International, 2015, 22: 752−756.

[19] NING Y Q, HUANG S B, FU M W, DONG J. Microstructural characterization, formation mechanism and fracture behavior of the needle δ phase in Fe−Ni−Cr type superalloys with high Nb content [J]. Materials Characterization, 2015, 109: 36−42.

[20] CHEN M S, ZOU Z H, LIN Y C, LI H B, WANG G Q, MA Y Y. Microstructural evolution and grain refinement mechanisms of a Ni-based superalloy during a two-stage annealing treatment [J]. Materials Characterization, 2019, 151: 445−456.

[21] LEE H T, HOU W H. Fine grains forming process, mechanism of fine grain formation and properties of superalloy 718 [J]. Materials Transactions, 2012, 53(4): 716−723.

[22] AGNOLI A, BERNACKI M, LOGÉ R, FRANCHET J M, LAIGO J, BOZZOLO N. Selective growth of low stored energy grains during δ sub-solvus annealing in the Inconel 718 nickel-based superalloy [J]. Metallurgical and Materials Transactions A, 2015, 46: 4405−4421.

[23] COLLIER J P, WONG S H. The effect of varying Al, Ti and Nb content on the phase stability of Inconel 718 [J]. Metallurgical Transactions A, 1988, 19: 1657−1668.

[24] LIU Yong-chang, ZHANG Hong-jun, GUO Qian-ying, ZHOU Xiao-sheng, MA Zong-qing, HUANG Yuan, LI Hui-jun. Microstructure evolution of Inconel 718 superalloy during hot working and its recent development tendency [J]. Acta Metallurgica Sinica−English Letters, 2018, 54(11): 1653−1664.

[25] WEI Xian-ping, ZHENG Wen-jie, SONG Zhi-gang, LEI Ting, YONG Qi-long, XIE Qing-cheng. Elemental partitioning characteristics of equilibrium phases in Inconel 718 alloy at 600−1100 °C [J]. Journal of Iron and Steel Research International, 2013, 20: 88−94.

[26] LI H Y, KONG Y H, CHEN G, XIE L X, ZHU S G, SHENG X. Effect of different processing technologies and heat treatments on the microstructure and creep behavior of GH4169 superalloy [J]. Materials Science and Engineering A, 2013, 582: 368−373.

[27] DENG Guo-jian, TU Shan-tung, ZHANG Xian-cheng, WANG Ji, ZHANG Cheng-cheng, QIAN Xia-yi, WANG Yi-ning. Small fatigue crack initiation and growth mechanisms of nickel-based superalloy GH4169 at 650 °C in air [J]. Engineering Fracture Mechanics, 2016, 153: 35−49.

[28] CONNOLLEY T, REED P A S, STARINK M J. Short crack initiation and growth at 600 °C in notched specimens of Inconel 718 [J]. Materials Science and Engineering A, 2003, 340: 139−154.

[29] RAMALHO MEDEIROS M A, HADAD C, PINTO A L, HENRIQUE L, ARAÚJO L S. The δ phase precipitation during processing and the influence on grain boundary character distribution and mechanical properties of superalloy 718 [J]. Materials Science and Engineering A, 2018, 726: 187−193.

[30] CHENG Miao, ZHANG Hong-hua, ZHANG Shao-ning. Microstructure evolution of delta-processed IN718 during holding period after hot deformation [J]. Journal of Materials Science, 2012, 47: 251−256.

冷轧细晶 GH4169 合金板材 δ 相析出规律及其对力学性能的影响

薛 浩[1]，赵静启[1]，刘永康[1]，张春祥[2]，骆俊廷[1,2]

1. 燕山大学 先进锻压成形技术与科学教育部重点实验室，秦皇岛 066004；
2. 燕山大学 亚稳材料制备技术与科学国家重点实验室，秦皇岛 066004

摘 要：采用冷轧和热处理对 GH4169 高温合金板材进行晶粒细化。研究冷轧压下率和热处理时间对 δ 析出相的影响，以及 δ 相含量和形貌对 GH4169 合金力学性能的影响。结果表明：冷轧变形可以促进 δ 相的析出，并促进 δ-Ni$_3$Nb 相转变为 δ-NbNi$_4$ 相。保温时间为 1 h 时，合金的综合性能较好，抗拉强度比未冷轧材料高 132 MPa，伸长率仅比未冷轧材料低 2.9%。合金的力学性能随 δ 相形貌的变化而产生较大改变。

关键词：细晶 GH4169 合金；冷轧；δ 相；力学性能

(Edited by Bing YANG)